

Uncovering the neutrino mass ordering with the next galactic core-collapse supernova neutrino burst

César Jesús-Valls^{1,*}

¹*Kavli IPMU (WPI), UTIAS, The University of Tokyo, Kashiwa, Chiba 277-8583, Japan*

A major conundrum of particle physics is what mass ordering (MO) follow neutrinos. The construction of next-generation neutrino detectors of unprecedented size, sensitivity and budget is underway and an answer is expected in the next decade through the combined study of reactor, atmospheric and accelerator neutrinos. In addition, due to the MSW effect the flavor content of the neutrino flux from a Core-Collapse Supernovae (CCSNe) is expected to be strongly dependent on the true neutrino MO. To exploit this feature, this Letter presents a novel analysis strategy robust to the most notable state-of-the-art systematic uncertainties arising from CCSN model-to-model neutrino flux variations and poorly known neutrino interaction cross-sections. By means of this method, is shown that for a paradigmatic galactic CCSN a great MO discrimination, similar to 5σ , could potentially be achieved.

INTRODUCTION

Neutrinos are essential ingredients of particle physics, astrophysics and cosmology, yet, some of their fundamental properties remain unknown. Under the most extended theoretical picture, consisting on the existence of three neutrino flavors able to mix, neutrino phenomenology is characterized by a set of seven degrees of freedom including three neutrino masses (m_1, m_2 and m_3) and four mixing parameters (θ_{12} , θ_{23} , θ_{13} and δ_{CP}). Currently, θ_{12} , θ_{23} , θ_{13} , $\delta m_{21}^2 (\equiv m_2^2 - m_1^2)$ and $|\Delta m_{32}^2| (\equiv |m_3^2 - m_2^2|)$ are known with few percent precision [1, 2] such that only three quantities remain elusive: a) the absolute neutrino mass scale, e.g. review [3], b) the value of δ_{CP} , e.g. refs. [2, 4] and c) the sign of Δm_{32}^2 , i.e. the so-called neutrino mass ordering (MO) that can be normal $m_2 < m_3$ (NMO) or inverted $m_3 < m_2$ (IMO). Regarding the MO, current data shows a statistical preference for the NMO of about 3σ [2]. Future experiments Hyper-Kamiokande [5], JUNO [6] and DUNE [7] will characterize the MO in detail via the study of atmospheric, reactor and accelerator neutrino oscillations. The complementarity of the above experiments is an attractive advantage: if all the MO results are consistent, it will reinforce the existing view of neutrino phenomenology, while the appearance of tensions in data could give us hints of new physics [8–10] requiring theoretical extensions. In the second scenario, having additional data would be particularly helpful in disentangling the true MO of new physical effects. In this sense, a unique opportunity would arise in the event of a galactic supernova (SN) neutrino burst [11–13].

CCSN per century is expected [16]. Consequently, so far only a couple dozen neutrinos have been detected from a single supernova, SN-1987a [17–20]. Nonetheless, the detection of SN-1987a confirmed our basic understanding of CCSN explosions and signified the start of experimental neutrino astrophysics. Furthermore, since the predicted neutrino flux and flavor composition are greatly influenced by a plethora of effects, the SN-1987a data was used to place significant limits on several exotic processes [21–25] and properties of neutrinos, including their mass [26, 27], magnetic moment [28] and mixing [29]. These achievements, however, are just a tantalizing hint of what might be possible with next-generation neutrino detectors. The increase of available data would be spectacular, e.g. $O(10^{4-6})$ detected neutrinos at Hyper-Kamiokande for a burst at a distance of 10-1 kpc [5]. Such a drastic improvement, however, would pose new challenges, in particular, the decrease in statistical error would force to shift the analysis focus towards the treatment and evaluation of systematic uncertainties, so far overlooked, in order to get the most from the precious supernova data.

In this Letter, attention is paid for the first time to role of the supernova model-to-model variations in the flux predictions and the uncertainty of neutrino interactions with bound nucleons when extracting physics parameters from supernova neutrinos. An analysis strategy robust to these uncertainties is identified, with the aim to uncover the neutrino MO using supernova neutrinos. The results prove that, for a paradigmatic galactic supernova, a strong statistical separation between both MOs could be achieved by analyzing the angular distribution of the reconstructed events.

Supernova neutrino bursts

Core collapse supernovae (CCSN) emit $O(10^{53})$ erg as neutrinos, i.e. $O(10^{58})$ neutrinos of $\langle E_\nu \rangle \sim 10$ MeV, in a ten-second burst [14, 15]. A low galactic rate of $3.2_{-2.6}^{+7.3}$

Neutrino flux predictions

The explosion mechanism of CCSN is still poorly understood [30]. However, the gradual increase in available computational power has allowed the set of

simplifying assumptions to be reduced over time, and in recent years CCSN models have begun to achieve realistic self-triggered explosions [30]. Furthermore, a general concordance has emerged in the neutrino flux predictions from different research teams [31–35]. New data from a future CCSN would be game-changing to better understand the dynamics of the explosion and to assess the reliability of the available models. Recently, first studies have shown that great CCSN model-discrimination could be achieved using Hyper-Kamiokande [5] (HK) or a HK-like detector [36]. This results might be potentially complemented with similar studies in JUNO [37] and DUNE [38] in the future.

Relevant interaction cross-sections

Supernova neutrinos have typical energies at the level of few tens of MeV [20]. At such energies, the main interactions with detector targets consists of neutrino- and antineutrino-electron elastic scattering (eES) [39], electron antineutrino inverse beta decay (IBD) [40] with unbound protons such as Hydrogen in water, and neutrino-nucleon charged- and neutral-current interactions with bound nucleons (e.g. ν_e -CC ^{16}O [41, 42]). Due to nuclear effects, neutrino interactions with bound nucleons are poorly known [43, 44], instead, eES and IBD predictions are expected to be accurate.

ANALYSIS STRATEGY

The analysis strategy consists in: 1) identifying a signature at the neutrino-flux level that is indicative of the true neutrino MO and robust across flux models 2) finding an observable that is sensitive to this feature 3) choosing a detector technology suitable to perform such a measurement 4) define an event selection criteria 5) estimate the total systematic uncertainty and 6) calculate the sensitivity to the neutrino MO using the former inputs.

Flux models

To study different flux models the SNEWPY [45, 46] open-source software package is used. The models under consideration are, following SNEWPY’s nomenclature, Bollig 2016 ($27 M_\odot$) [47], Warren 2020 ($13 M_\odot$) [48] Fornax 2021 ($20 M_\odot$) [30], Zha 2021 ($16 M_\odot$) [49]. This choice aims to use relatively new models, less tied to simplifying assumptions than older versions, spanning a wide range of progenitor masses and that last a time-lapse long enough to accumulate a significant number of events. Accordingly, the first 2 s of the explosion will be studied since that is the shortest simulated time span

among all models under studyⁱ.

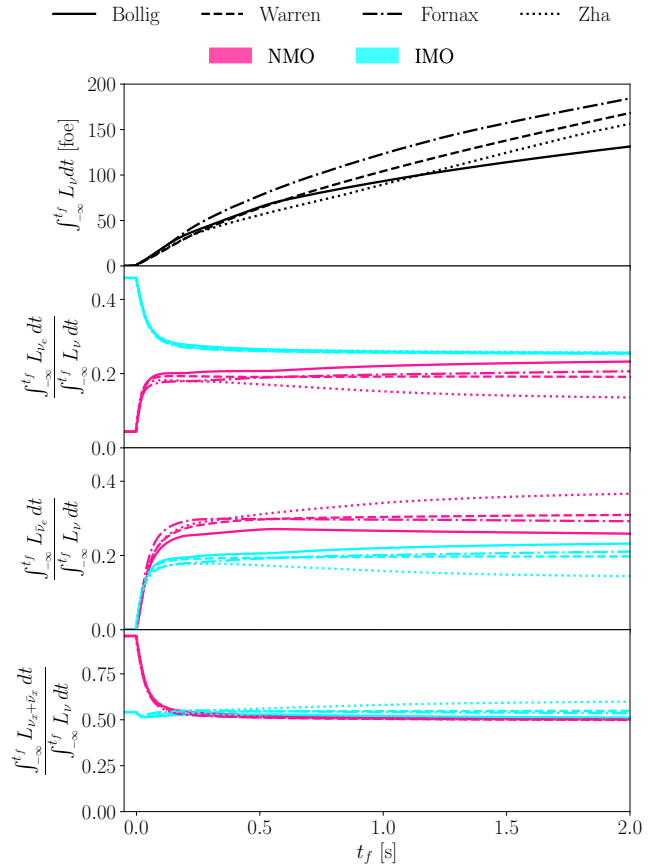


FIG. 1: Total neutrino flux and relative flavor fractions integrated over a time-lapse ranging from the start of the SN explosion, denoted by $-\infty$, until a final time, t_f , for the different flux models presented in the text.

In CCSN, the neutrino flux flavor composition is influenced by the Mikheyev–Smirnov–Wolfenstein (MSW) effect [50, 51]. If $\sin^2 \theta_{13} > 10^{-3}$, as it is indeed the case [52], a non-oscillatory adiabatic flavor conversion, sensitive to the neutrino MO, is expected [53]. To describe this effect, the neutrino flux is modified according to **AdiabaticMSW** transformationsⁱⁱ using SNEWPY. These transformations depend on θ_{13} and θ_{23} [11], with values chosen from the Particle Data Group [54]. Since the uncertainty on these parameters is small the variations inflicted to the expected flavor predictions are minor, specially when compared to CCSN model-to-model variations. Hence, the uncertainty on these parameters is neglected, such as in Ref. [5]. It is worth noting that effects yet poorly understood, such as fast pairwise flavor conversions [55–57] and flavor angular anisotropies [58],

ⁱ This constrain is imposed by the Zha 2021 ($16 M_\odot$) [49] model.

ⁱⁱ Implementation details are available in Appendix A of Ref. [45].

might change the state-of-the-art CCSN model neutrino flavor predictions. Hence, future advances on the theoretical understanding of these processes and the proliferation of available multi-second simulation explosions would be greatly beneficial to increase the robustness of any study that aims to extract physics conclusions by comparing CCSN model predictions and data.

Neutrino flux models, see Fig. 1, have the neutrino luminosity divided into four flavor categories: L_{ν_e} , $L_{\bar{\nu}_e}$, L_{ν_x} and $L_{\bar{\nu}_x}$, where $x \equiv \mu + \tau$. The time evolution of the supernova explosion is markedly different between models such that $L(t)$ is not a model-robust observable. This is also true for the total neutrino luminosity integrated over time, i.e., $\int L_\nu(t) dt$ due to, among other effects, scale differences, e.g., the progenitor mass. However, as presented in see Fig. 1, the time-integrated fraction of different flavors is consistently different as a function of the true neutrino MO across flux models.

Since each model uses a different time reference definition, small time offsets are applied by setting the t_0 of each model as the time at which the neutrino luminosity reaches its maximum. Notably, this time frame could also be set for data analyzing the time spectrum of events. Although this calculation would introduce an associated detector systematic uncertainty, its role is later neglected as it would be, arguablyⁱⁱⁱ, a sub-leading correction.

Observable definition

To be sensitive to the MO, it is necessary to find an observable that changes with the flux flavor content such that the differences presented in the former section can be sized. Among the interaction channels listed in Sec. all flavors contribute equally to eES whereas IBD is only possible for $\bar{\nu}_e$. Therefore, a measurement able to discriminate one reaction from the other is directly informative of the flux flavor and therefore of the true neutrino MO. It is well known that electrons emitted in eES are peaked forward whereas those from IBD and CC- ^{16}O are almost isotropic, as illustrated in Fig. 2. This feature has been used for years in the study of solar neutrinos [59] and provides the best known strategy to reconstruct the CCSN position in the sky [60]. Here, we extend the use of this feature to study the neutrino MO by noting that the expected shape of the angular distribution of outgoing e^\pm is strongly influenced by the flux flavor content and therefore by the true neutrino MO.

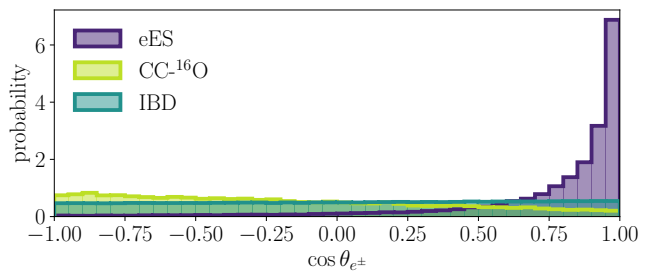


FIG. 2: Binned probability density function of the reconstructed angle for outgoing electrons and positrons, split by interaction channel, generated for neutrino interactions in water using the **Warren** flux model, presented in the text, transformed by **AdiabaticMSW** for the NMO.

Detector choice

Among the existing and planned neutrino telescopes, the Hyper-Kamiokande detector (HK) [60] is the best suited detector to study the angular distribution of SN neutrinos. Therefore, its specifications are used for the analysis that follows. The motivations behind this choice are:

- HK will be a water Cherenkov detector, a well understood technology. It is expected to become operational in 2027 and preparations are on schedule. With a huge fiducial mass of 187 kT it would collect an enormous number of events compared to other experiments with masses of the order of a few tens of kT, such as its predecessor, Super-Kamiokande and the future experiments JUNO and DUNE.
- HK will be able to analyze individual events and will have excellent angular reconstruction capabilities; requirements that rule out the JUNO and IceCube [61] experiments for this analysis.
- At HK, due to the presence of Hydrogen in water only a very small fraction of the interactions would occur with bound nucleons [5], reducing the impact of cross-section uncertainties. This situation contrasts with that of DUNE where most of the interactions would be with Argon nucleons [38].
- HK performances can be reliably modeled using Super-Kamiokande IV [59] as a lower bound.

Event simulation and selection criteria

To translate neutrino luminosities into event rates the **sntools** [62] open-source software package is used. **sntools** reads fluxes in **SNEWPY** format and combines them with neutrino cross-sections to generate realistic

ⁱⁱⁱ If a low number of interactions are recorded, statistical errors dominate. Else, σ_{t_0} could be determined with few milliseconds precision from the interactions time spectrum. Thus, $\sigma_{t_0} \ll 2$ s would translate into a tiny variation of the integrated flavor composition and therefore into a minor systematic uncertainty.

event rates and particle distributions using Monte Carlo sampling.

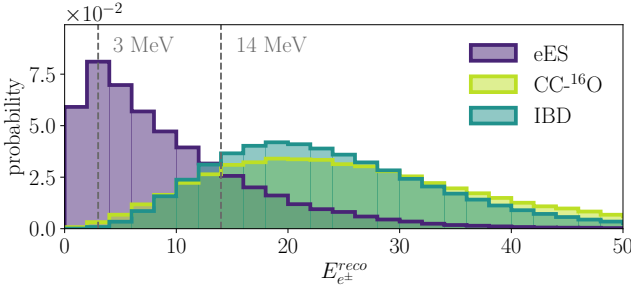


FIG. 3: Binned probability density function of the reconstructed energy for outgoing electrons and positrons, split by interaction channel, generated for neutrino interactions in water using the **Warren** flux model, presented in the text, transformed by **AdiabaticMSW** for the NMO.

Cuts	NMO			IMO		
	IBD [%]	eES [%]	^{16}O [%]	IBD [%]	eES [%]	^{16}O [%]
A	90.2 ± 2.3	4.3 ± 1.0	5.5 ± 2.5	86.0 ± 3.3	6.7 ± 1.0	7.3 ± 3.2
B	91.0 ± 2.3	3.4 ± 0.8	5.5 ± 2.5	87.2 ± 3.3	5.4 ± 0.9	7.4 ± 3.2
C	83.6 ± 0.4	12.8 ± 0.5	3.6 ± 0.5	75.6 ± 4.2	20.0 ± 3.2	4.5 ± 1.0

TABLE I: Fractions of selected interactions in HK after applying the cuts *A*, *B* and *C*, corresponding to: *A*) No cuts; *B*) $E_{e^\pm}^{\text{reco}} > 3$ MeV and *C*) $14 > E_{e^\pm}^{\text{reco}} > 3$ MeV. The intervals reflect the mean and standard deviation of the values found across the flux models in Sec. .

A million events is simulated for each SN model and MO and the expected angular distribution of the outgoing e^\pm is computed relative to the SN direction. To make the analysis robust to scale differences the distribution is normalized to unity. To obtain realistic distributions, the true θ_{e^\pm} and E_{e^\pm} are smeared using the reconstruction capabilities of Super-Kamiokande IV [59], which set a lower bound for HK performances. Then, events with $E^{\text{max}} > E_{e^\pm}^{\text{reco}} > 3$ MeV are selected. This choice aims to: 1) account for a realistic detection energy threshold^{iv} and 2) increase (decrease) the fraction of eES (CC- ^{16}O), which is concentrated at low (high) energies, see Fig. 3, and reduce the flux model-to-model discrepancies, particularly relevant at high $E_{e^\pm}^{\text{reco}}$. While aggressive cuts on E^{max} improve the model robustness, they reduce the number of selected events and therefore increase the statistical error. To balance such a trade-off,

$E^{\text{max}} = 14$ MeV was chosen as it provides maximum MO sensitivity^v. After the cuts, the interaction fractions change as summarized in Tab. I. As it can be seen, the cuts significantly reduce the variation of the predictions across flux models, decrease the fraction of CC- ^{16}O and significantly increase the proportion of eES events. As intended, the separation of NMO and IMO predictions is significantly accentuated by using a high-energy cut.

Evaluation of uncertainties

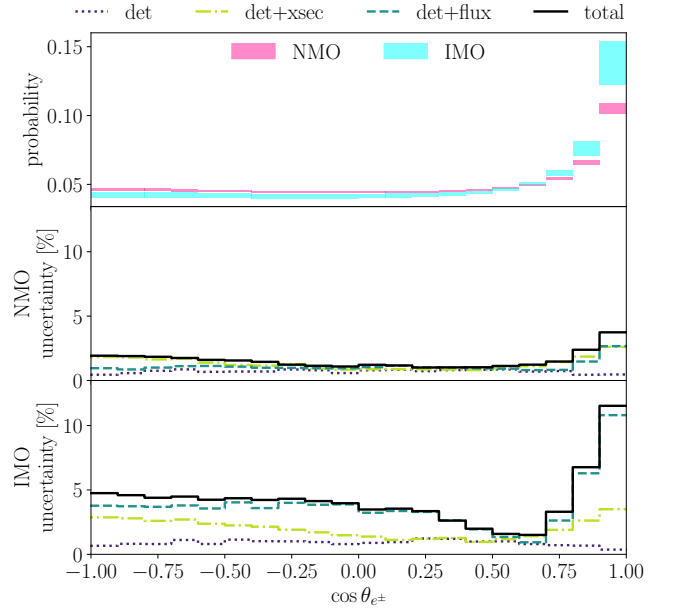


FIG. 4: Binned probability of the expected angular distribution for both MOs. Each bin is represented as a colorbox covering 1σ of the total uncertainty. Central and bottom panels: break-down of the uncertainty for each MO in terms of its detector-only (*det*), detector and cross-section (*det+xsec*), and detector and flux (*det+flux*) systematic uncertainties.

To account for the cross-section model uncertainties, the weight associated to all selected CC- ^{16}O is varied assuming a 100% normalization uncertainty^{vi}. For each MO and toy configuration, i.e., a particular instance of a flux model, collection of smeared angles and energies,

^{iv} In SK-IV a threshold as low as 3.49 MeV was used to study solar neutrinos [59]. Hyper-Kamiokande expects to detect 10 photo-electrons/MeV compared to the 6 photo-electrons/MeV at SK-IV [63]. Thus, a 3 MeV threshold is assumed.

^v The whole analysis chain was re-run to test several values of E^{max} , in steps of 1 MeV. Cuts in time were also studied, but it was observed that using the full 2 s windows lead to the best sensitivity, so no additional restrictions were applied.

^{vi} The absence of experimental data prevents the use of a more specific choice. The value of 100% is a usual conservative choice when a normalization constrain is missing.

and cross-section weights the resulting normalized angular distribution is calculated. The mean of all distributions and its standard deviation corresponds to the expected angular distribution and its associated uncertainty. This is presented in the top panel of Fig. 4.

To get some insight on the nature of the total error budget the size of individual contributions is studied. To quantify the role of detector uncertainties all cross-section weights are set to one and calculated individually for each flux model. The flux-averaged detector uncertainty (*det*) is calculated as the mean of the spreads across flux models. The process is repeated, this time varying at the same time the cross-section weights, leading to a detector plus cross-section uncertainty averaged across flux models (*det+xsec*). Finally, the cross-section weights are set to one, and the variation across detector effects and flux models (*det+flux*) is calculated. It is worth noting that, since reconstructed variables are used, cross-section and flux model uncertainties are intertwined with detector effects and, consequently, *det+xsec* and *det+flux* are reported together. The results are presented in the central and bottom panel of Fig. 4. As it can be seen, the dominant contribution is that of flux model differences followed by cross-section effects.

In the future, it might be possible to shrink the flux and cross-section uncertainties if: 1) The SN explosion mechanism is better understood and the results of different groups continue to converge and 2) model predictions for low energy, i.e. $O(10)$ MeV, neutrino-nucleus interactions can be compared to data. The state-of-the-art of neutrino research, very active on both of the former topics, makes it possible to expect updates in the near future.

The statistical uncertainty (σ_{stat}) can be straightforwardly computed distributing a number of selected neutrinos, N^{sel} , according to the distributions in the top panel of Fig. 4 and sizing the variations using Poisson statistics. To calculate the total error budget the statistical and systematic uncertainties (σ_{syst}) are added in quadrature ($\sigma_{stat} \oplus \sigma_{syst}$).

Sensitivity calculation

The sensitivity corresponds to the statistical separation between both MOs. To calculate it, the following method is used:

- A MO is assumed, i.e., the NMO.
- A number of selected SN neutrino interactions, N^{sel} , is chosen.
- A set of 50k toys are generated. Each toy corresponds to sample Gaussianly the value of each bin from the assumed MO mean and total uncertainty.

- For each toy, χ_{NMO}^2 and χ_{IMO}^2 are calculated using

$$\chi_M^2 = \sum_i^{bins} \frac{(\mu^i - \hat{\mu}_M^i)^2}{\sigma_M^2}, \quad \chi_M^2 = \{\chi_{NMO}^2, \chi_{IMO}^2\} \quad (1)$$

where $\hat{\mu}_M^i$, μ^i and σ_M^i are respectively the expected value, the toy value and the uncertainty at the i -th bin for the mass ordering M .

- $\Delta\chi^2$ is calculated, defined as $\Delta\chi^2 \equiv \chi_{NMO}^2 - \chi_{IMO}^2$.
- The distribution of $\Delta\chi^2$ for all toys is fit with a Gaussian. By, definition, positive (negative) values are indicative of the NMO (IMO). To obtain the sensitivity of correctly assessing the MO the fit is integrated from $-\infty$ to 0. Finally, the p-value is converted into σ .

SENSITIVITY AND OUTLOOK

Using the above method the sensitivity to identify the true MO is calculated for a number of selected neutrinos in the interval from 1k to 15k. The results are presented in Fig. 5. To isolate the contribution of systematic uncertainties, the results are presented both for σ_{stat} only and for $\sigma_{stat} \oplus \sigma_{syst}$. To provide some intuition on the expected number of selected neutrinos, lines with the expectation for all models, assuming the NMO at the average galactic distance of 10 kpc, are included. As can be seen on the plot, a sensitivity similar to 5σ is reached for 10 kpc for all models. If the IMO is realized in nature, a smaller number of selected neutrinos is expected. For 10 kpc and the flux models under consideration, this number would be about 5.6k selected neutrinos, or equivalently, a sensitivity similar to 4σ . For the most distant stars in the galactic plane, at about 20 kpc, the number of selected events would be reduced to $1/4$, hence resulting in sensitivities similar to 3σ .

Summing up, the results show that: 1) the time-integrated flavor content is a flux-model robust quantity indicative of the true neutrino MO; 2) the shape of the angular distribution of outgoing e^\pm is a sensible observable to study the flavor composition of a SN neutrino flux; 3) The Hyper-Kamiokande detector is a well suited technology for that analysis thanks to the presence of free nucleons in water that mitigate the role of cross-section uncertainties, its expected excellent pointing capabilities and its large mass; 4) the current level of systematic uncertainties affects the shape-only predictions at the few percent level; 5) for typical galactic distances a large sensitivity to the true neutrino MO can be expected, similar to 3σ at the edge of the galactic disk (20 kpc), of 4-5 σ for typical distances (10 kpc) and beyond 5σ for nearby SN explosions.

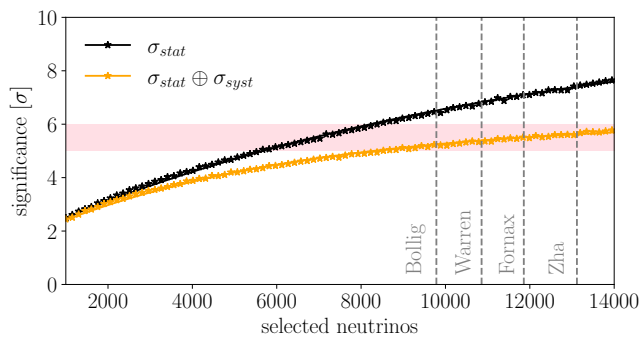


FIG. 5: Sensitivity to the true neutrino MO as a function of the number of neutrinos selected with the criteria discussed in the text. The 4-5 σ band is highlighted using a red shadow and vertical dashed lines illustrate the number of expected selected neutrinos assuming the NMO for all models used in the analysis at the average galactic plane distance of 10 kpc.

ACKNOWLEDGMENTS

The author is indebted to CERN for organizing the INSS where the idea of this project was first sparked and acknowledges fruitful discussions with T. Lux, E. Ramos-Cascón and P. Barham, the help of J. Migenda to install SNEWPY and sntools and the feedback on the manuscript from C. Alt, S. Dolan and S. Julià-Farré.

* E-mail: cesar.jesus-valls@ipmu.jp

- [1] P. F. de Salas, D. V. Forero, S. Gariazzo, P. Martínez-Miravé, O. Mena, C. A. Ternes, M. Tórtola, and J. W. F. Valle, JHEP **02**, 071 (2021), arXiv:2006.11237 [hep-ph].
- [2] I. Esteban, M. C. Gonzalez-Garcia, M. Maltoni, T. Schwetz, and A. Zhou, JHEP **09**, 178 (2020), arXiv:2007.14792 [hep-ph].
- [3] J. A. Formaggio, A. L. C. de Gouvêa, and R. G. H. Robertson, Phys. Rept. **914**, 1 (2021), arXiv:2102.00594 [nucl-ex].
- [4] K. Abe *et al.* (T2K), Nature **580**, 339 (2020), [Erratum: Nature 583, E16 (2020)], arXiv:1910.03887 [hep-ex].
- [5] K. Abe *et al.* (Hyper-Kamiokande), Astrophys. J. **916**, 15 (2021), arXiv:2101.05269 [astro-ph.IM].
- [6] F. An *et al.* (JUNO), J. Phys. G **43**, 030401 (2016), arXiv:1507.05613 [physics.ins-det].
- [7] B. Abi *et al.* (DUNE), (2020), arXiv:2002.03005 [hep-ex].
- [8] P. B. Denton, J. Gehrlein, and R. Pestes, Phys. Rev. Lett. **126**, 051801 (2021), arXiv:2008.01110 [hep-ph].
- [9] S. S. Chatterjee and A. Palazzo, Phys. Rev. Lett. **126**, 051802 (2021), arXiv:2008.04161 [hep-ph].
- [10] P.-W. Chang, I. Esteban, J. F. Beacom, T. A. Thompson, and C. M. Hirata, (2022), arXiv:2206.12426 [hep-ph].
- [11] A. S. Dighe and A. Y. Smirnov, Phys. Rev. D **62**, 033007 (2000), arXiv:hep-ph/9907423.
- [12] K. Scholberg, J. Phys. G **45**, 014002 (2018), arXiv:1707.06384 [hep-ex].
- [13] V. Brdar and X.-J. Xu, JCAP **08**, 067 (2022), arXiv:2204.13135 [hep-ph].
- [14] S. W. Barwick *et al.*, (2004), arXiv:astro-ph/0412544.
- [15] H.-T. Janka, Ann. Rev. Nucl. Part. Sci. **62**, 407 (2012), arXiv:1206.2503 [astro-ph.SR].
- [16] S. M. Adams, C. S. Kochanek, J. F. Beacom, M. R. Vagins, and K. Z. Stanek, Astrophys. J. **778**, 164 (2013), arXiv:1306.0559 [astro-ph.HE].
- [17] K. Hirata *et al.* (Kamiokande-II), Phys. Rev. Lett. **58**, 1490 (1987).
- [18] K. S. Hirata *et al.*, Phys. Rev. D **38**, 448 (1988).
- [19] R. M. Bionta *et al.*, Phys. Rev. Lett. **58**, 1494 (1987).
- [20] H. A. Bethe, Rev. Mod. Phys. **62**, 801 (1990).
- [21] G. Raffelt and D. Seckel, Phys. Rev. Lett. **60**, 1793 (1988).
- [22] M. S. Turner, Phys. Rev. Lett. **60**, 1797 (1988).
- [23] G. G. Raffelt, Lect. Notes Phys. **741**, 51 (2008), arXiv:hep-ph/0611350.
- [24] J. H. Chang, R. Essig, and S. D. McDermott, JHEP **01**, 107 (2017), arXiv:1611.03864 [hep-ph].
- [25] J. H. Chang, R. Essig, and S. D. McDermott, JHEP **09**, 051 (2018), arXiv:1803.00993 [hep-ph].
- [26] J. N. Bahcall and S. L. Glashow, Nature **326**, 476 (1987).
- [27] D. N. Spergel and J. N. Bahcall, Phys. Lett. B **200**, 366 (1988).
- [28] R. Barbieri and R. N. Mohapatra, Phys. Rev. Lett. **61**, 27 (1988).
- [29] B. Jegerlehner, F. Neubig, and G. Raffelt, Phys. Rev. D **54**, 1194 (1996), arXiv:astro-ph/9601111.
- [30] A. Burrows and D. Vartanyan, Nature **589**, 29 (2021), arXiv:2009.14157 [astro-ph.SR].
- [31] E. J. Lentz, S. W. Bruenn, W. R. Hix, A. Mezzacappa, O. E. B. Messer, E. Endeve, J. M. Blondin, J. A. Harris, P. Marronetti, and K. N. Yakunin, Astrophys. J. Lett. **807**, L31 (2015), arXiv:1505.05110 [astro-ph.SR].
- [32] T. Melson, H.-T. Janka, and A. Marek, Astrophys. J. Lett. **801**, L24 (2015), arXiv:1501.01961 [astro-ph.SR].
- [33] M. A. Skinner, J. C. Dolence, A. Burrows, D. Radice, and D. Vartanyan, Astrophys. J. Suppl. **241**, 7 (2019), arXiv:1806.07390 [astro-ph.IM].
- [34] E. P. O'Connor and S. M. Couch, Astrophys. J. **865**, 81 (2018), arXiv:1807.07579 [astro-ph.HE].
- [35] T. Kuroda, A. Arcones, T. Takiwaki, and K. Kotake, Astrophys. J. **896**, 102 (2020), arXiv:2003.02004 [astro-ph.HE].
- [36] J. Olsen and Y.-Z. Qian, Phys. Rev. D **105**, 083017 (2022), arXiv:2202.09975 [astro-ph.HE].
- [37] T. Birkenfeld (JUNO), PoS **ICHEP2020**, 619 (2021).
- [38] B. Abi *et al.* (DUNE), Eur. Phys. J. C **81**, 423 (2021), arXiv:2008.06647 [hep-ex].
- [39] J. N. Bahcall, M. Kamionkowski, and A. Sirlin, Phys. Rev. D **51**, 6146 (1995), arXiv:astro-ph/9502003.
- [40] A. Strumia and F. Vissani, Phys. Lett. B **564**, 42 (2003), arXiv:astro-ph/0302055.
- [41] T. Suzuki, S. Chiba, T. Yoshida, K. Takahashi, and H. Umeda, Phys. Rev. C **98**, 034613 (2018), arXiv:1807.02367 [nucl-th].
- [42] K. Nakazato, T. Suzuki, and M. Sakuda, PTEP **2018**, 123E02 (2018), arXiv:1809.08398 [astro-ph.HE].
- [43] N. Van Dessel, A. Nikolakopoulos, and N. Jachowicz, Phys. Rev. C **101**, 045502 (2020), arXiv:1912.10714 [nucl-th].
- [44] S. Gardiner, Phys. Rev. C **103**, 044604 (2021), arXiv:2010.02393 [nucl-th].

- [45] A. L. Baxter *et al.* (SNEWS), *Astrophys. J.* **925**, 107 (2022), arXiv:2109.08188 [astro-ph.IM].
- [46] A. Baxter *et al.*, *J. Open Source Softw.* **6**, 3772 (2021).
- [47] A. Mirizzi, I. Tamborra, H.-T. Janka, N. Saviano, K. Scholberg, R. Bollig, L. Hudepohl, and S. Chakraborty, *Riv. Nuovo Cim.* **39**, 1 (2016), arXiv:1508.00785 [astro-ph.HE].
- [48] M. L. Warren, S. M. Couch, E. P. O'Connor, and V. Morozova, *Astrophys. J.* **898**, 139 (2020), arXiv:1912.03328 [astro-ph.HE].
- [49] S. Zha, E. P. O'Connor, and A. da Silva Schneider, *Astrophys. J.* **911**, 74 (2021), arXiv:2103.02268 [astro-ph.HE].
- [50] S. P. Mikheyev and A. Y. Smirnov, *Sov. J. Nucl. Phys.* **42**, 913 (1985).
- [51] L. Wolfenstein, *Phys. Rev. D* **17**, 2369 (1978).
- [52] P. A. Zyla *et al.* (Particle Data Group), *PTEP* **2020**, 083C01 (2020).
- [53] A. Y. Smirnov, *Phys. Scripta T* **121**, 57 (2005), arXiv:hep-ph/0412391.
- [54] M. Tanabashi *et al.* (Particle Data Group), *Phys. Rev. D* **98**, 030001 (2018).
- [55] R. F. Sawyer, *Phys. Rev. D* **72**, 045003 (2005), arXiv:hep-ph/0503013.
- [56] H. Nagakura, L. Johns, A. Burrows, and G. M. Fuller, *Phys. Rev. D* **104**, 083025 (2021), arXiv:2108.07281 [astro-ph.HE].
- [57] I. Padilla-Gay, I. Tamborra, and G. G. Raffelt, *Phys. Rev. Lett.* **128**, 121102 (2022), arXiv:2109.14627 [astro-ph.HE].
- [58] H. Nagakura, A. Burrows, D. Vartanyan, and D. Radice, *Monthly Notices of the Royal Astronomical Society* **500**, 696 (2021).
- [59] K. Abe *et al.* (Super-Kamiokande), *Phys. Rev. D* **94**, 052010 (2016), arXiv:1606.07538 [hep-ex].
- [60] K. Abe *et al.* (Hyper-Kamiokande), (2018), arXiv:1805.04163 [physics.ins-det].
- [61] M. G. Aartsen *et al.* (IceCube), *JINST* **12**, P03012 (2017), arXiv:1612.05093 [astro-ph.IM].
- [62] J. Migenda, S. Cartwright, L. Kneale, M. Malek, Y.-J. Schnellbach, and O. Stone, *J. Open Source Softw.* **6**, 2877 (2021).
- [63] J. Bian *et al.* (Hyper-Kamiokande), in *2022 Snowmass Summer Study* (2022) arXiv:2203.02029 [hep-ex].